DYNAMIC RESPONSE OF STEEL SPECIMEN UNDER DEBRIS FLOW SURGE MODEL

Nobutaka Ishikawa[1],Ryuta Inoue[2], Masuhiro Beppu[3],Yuji Hasegawa[4], Takahisa Mizuyama[5]

ABSTRACT

This paper presents experimental and analytical approaches on the dynamic load and the dynamic response of a dam structure model under debris flow models. First, the dynamic load test is performed in order to find the impulsive fluid load showing the surge shape among three different types of debris flow models by using the hydrodynamic channel. It was found that the impulsive shape was well formed at the debris flow model with the ratio of 70% gravel and 30% sand. Second, the dynamic response test is executed for dam models under impulsive load. It was recognized that the dynamic response of steel plate showed a ductile behaviour against impulsive load, even a thin steel plate. Finally, the particle method is applied to dynamic response of a steel plate under water flow. It was noted that the particle method (MPS method) could simulate well the dynamic load and dynamic response of a steel plate under water flow.

Keywords: debris flow, dynamic response, Sabo dam model, particle method, surge shape

INTRODUCTION

Recently many debris flow disasters have occurred due to torrential rainfall as a result of the abnormal weather. Some disasters may be due to the impulsive fluid load of surge debris flow. Many studies (Bugnion (2011), Daido (1988), Hirao (1970), Horii (2002), Hu (2011), Mizuyama (1979,1985), Miyamoto (1983), Miyoshi (1990)) have devoted to the impulsive load of debris flow based on the dynamic fluid theory. Authors (2008, 2009, 2010) have also examined the dynamic load of debris flow model in order to reproduce the surge formation. However, few studies have been done on the dynamic response of the structure under an impulsive debris flow. Therefore, the objective of this study is to investigate the dynamic response of a dam structure under an impulsive debris flow. To this end, this paper presents experimental and analytical approaches on the dynamic response of Sabo dam model under debris flow models.

First, the dynamic load test is performed by providing for three different types of debris flow models in the hydrodynamic channel. The objective of load test is to examine the possibility of surge formation showing impulsive load. Herein, the dynamic load-time relations of these debris flow models are obtained by the load cell synchronizing with the high speed video camera. Second, the dynamic response test is executed by using Sabo dam models (steel and mortal plates) under debris flow surge model. Herein, the strain and deformation-time relations of dam models are obtained by using the strain gages and the laser type deformation sensor, respectively.

Finally, the dynamic response analysis of a steel plate is performed by combining the particle method (MPS (Moving Particle Semi-implicit) method) with the deformation analysis of a beam member (a cantilever beam) under a debris flow model (water flow). The computational results are compared with the test results of the load, deformation and strain-time relations.

[1] Research Advisor, Research Association for Steel Sabo Structures, 2-7-5 Hirakawa-cho, Chiyoda-ku, Tokyo,102-0093, Japan (e-mail:cgishikawa@m4.dion.ne.jp)
2 Civil Engineer, Kyosei-Kiko,1-23-1 Shinjyuku-ku, Tokyo160-0022,Japan
3 Associate Professor, Department of Civil and Environmental Engineering, National Defense Academy, 1-10-20 Hashirimizu, Yokosuka 239-8686, Japan
4 Senior Researcher, Civil Engineering Research Laboratory, 904-1 Tohhigashi, Ibaraki,300-2633,Japan
5 Professor, Department of Erosion and Control Engineering, Graduate School of Agriculture, Kyoto University, Kitashirakawa, Oiwake-cho, Sakyo-ku, Kyoto, 606-8502, Japan

DYNAMIC LOAD TEST

Outline of test

The dynamic load test is performed for three different types of debris flow models in order to reproduce the surge formation by using the hydrodynamic channel.

The hydrodynamic channel test is performed with the slope of 18 degrees and the channel width of 10cm as shown in Fig.1(a). The measurement system of dynamic fluid load is illustrated as shown in Fig.1(b). By pouring water of 2 ℓ/sec into the debris flow model which is piling up to the washout height beforehand, the debris flow model flows at the instance of taking off the stopping panel as shown in Fig.2. The rib roughness is set up in the flow floor at the flow distance of 5.0m in order to reproduce the occurrence field of debris flow.

(a) Hydrodynamic channel

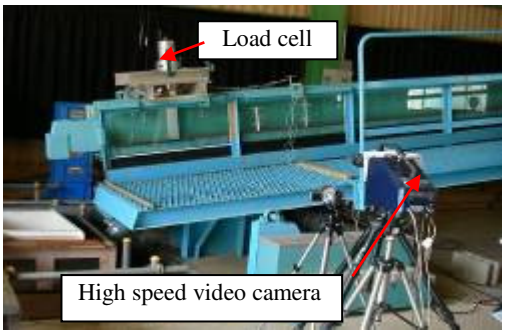

(b) Measurement system

Fig. 1 Experimental apparatus set-up

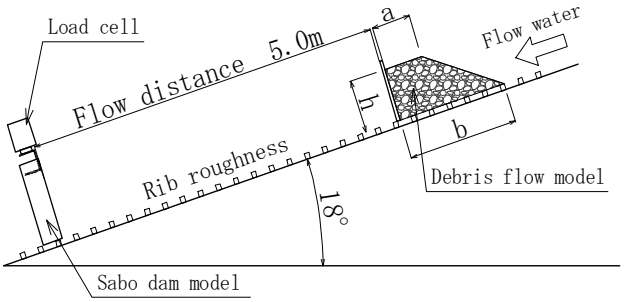

Fig.2 Dynamic load test

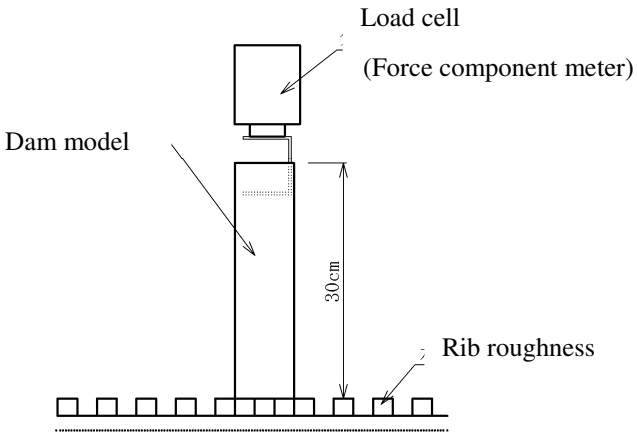

Fig. 3 Measurement of dynamic load

Debris flow model

The debris flow models were provided by using the water only and two different gravel size distributions adopting the natural materials. That is,

Type A: water,

Type B: the ratio of 70% gravel (16-19mm) and 30% sand (less than 2mm),

Type C: the ratio of 30% gravel (16-19mm) and 70% sand (less than 2mm).

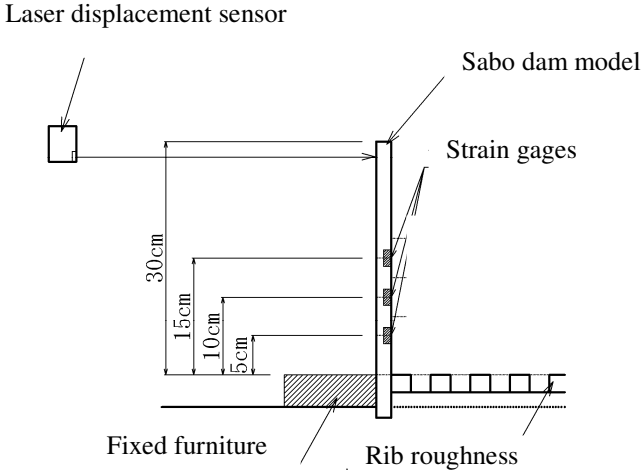

Fig.4 Measurement of dynamic response

Sabo dam model

The Sabo dam model is made by the steel specimen with the width of 100mm , the length of 300mm and the thickness of 20mm in case of the dynamic load test.

Measurement system

The dynamic fluid load is measured by the load cell (force component meter with sampling frequency of 1kHz)
as shown in Fig.3, synchronizing with the high speed video camera to take the front motion as shown in Fig.1(b).
The strains and deformation of plates are measured by using strain gages and laser displacement sensor, respectively, as shown in Fig.4.

Dynamic load test case

The dynamic load test was performed twice for each Type to examine if the surge shape could be formed among three different types of debris flow model or not.

Dynamic load test results

The load-time relations of Types A, B and C are shown in Fig.5.
Type A (water flow) has no clear peak load in the load-time relation and the precise surge formation was not seen in the front motion as shown in Fig.6(a).
Type B (gravel 7: sand 3) illustrates the very steep rise time in the load-time relation and the complete surge shape is formed in the front flow motion as shown in Fig.6(b).
Type C (gravel 3: sand 7) has very slow rise time in the load-time relation and the surge formation was not so clearly found in the front motion as shown in Fig.6(c).

The dynamic load test results are shown in Tab.1.

(1) Surge formation

In order to examine the dynamic load characteristics of Types A,B,C, the load ratio is defined as $P^* = P_{max}/P$ (P_{max}: peak load, P: constant load) and the surge formation is judged from the viewpoint of the load ratio as follows (Ishikawa,2010):

$P^* > 1.5$; complete surge formation (1a)
$1.0 \leq P^* \leq 1.5$; quasi surge formation (1b)
$P^* \leq 1.0$; no surge formation (1c)

It was noted from Tab.1 that the ratio of Type A was P^*=1.0-1.2, and, therefore,Type A was a quasi surge formation far from the complete surge formation.
It was found that the ratio of Type B was $P^* = P_{max}/P > 1.7$ and, as such, Type B was the complete surge formation which had the same tendency as the previous study (Ishikawa 2010). This reason will be explained later.

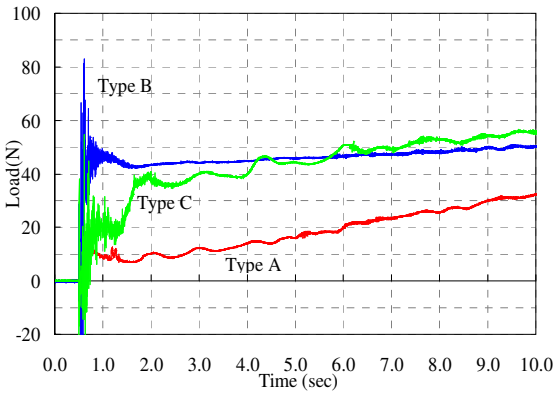

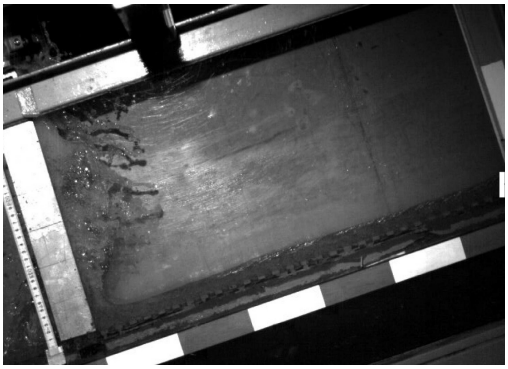

(a) Type A (water flow)

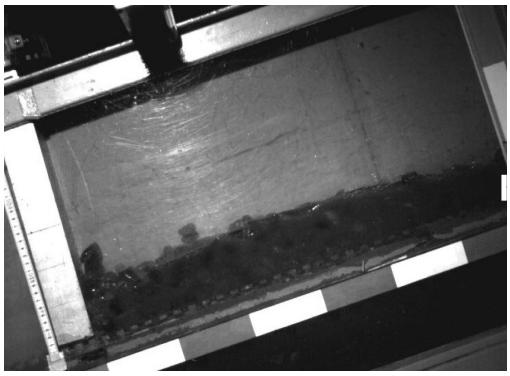

(b) Type B (gravel 7: sand 3)

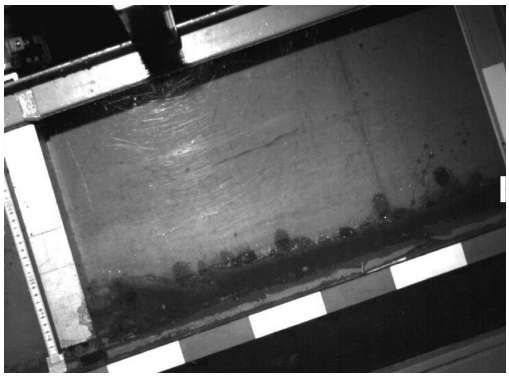

(c) Type C (gravel 3 : sand 7)

Fig. 6 Front motions of debris flow models (correspond to the peak load in Fig.5)

As the ratio of Type C was P^*=1.3-1.7, it was judged as a quasi surge formation.
Consequently, it was recognized that the debris flow model of Type B including 70% gravel and 30% sand could form the complete surge phenomenon exhibiting the impulsive fluid load which shows the very steep rise time in the load-time relation in Fig.5 and the large load ratio $P^*=P_{max}/P$ in Tab.1. It is also noted that the Froude number was F_r=2.1-2.4 in Type B which was the smallest among the debris flow models.This means that the surge of deberis flow may be easily formed when the water depth is large and the flow velocity is relatively slow.

(2) Comparison of design load with constant load after peak load

The design load ($F=\rho Av^2$, ρ: debris flow density, A: sectional area, v: flow velocity) is computed by using test data (flow velocity and water depth) and is compared with the constant load P after the peak load as shown in Tab.1. Herein, ρ=1.0-1.55g/cm^3, A=300cm^2, v=1.61-2.70m/sec were used .
As the results of computation of $F^*=F/P$, the values F^* of Types A and Type B were almost 1.0 (F^*=0.92-1.03 and F^*=0.91-0.97 except 0.59). However, in case of Type C (F^*=0.24-0.26), the design load F does not coincide with the constant load P, because the water depth and flow velocity were not stabilized by the effect of gravel size distribution with 30% gravel and 70% sand.

Tab.1 Dynamic load test results

No	Debris flow model density ρ(g/cm^3)	Peak load P_{max}(N)	Constant load P(N)	Flow velocity v(m/sec)	Water depth h(cm)	Design load F(N)	$F^*=\frac{F}{P}$	$P^*=\frac{P_{max}}{P}$	Froude number $F_r=v/\sqrt{hg}$
1	Type A 1.00	12.0	10.0	2.33	1.7	9.2	0.92	1.20	5.7
2	Type A 1.00	11.2	9.4	2.36	1.7	9.5	1.01	1.19	5.8
3	Type A 1.00	12.5	12.0	2.70	1.7	12.4	1.03	1.04	6.6
4	Type B 1.55	82.0	42.0	1.92	6.7	38.3	0.91	1.95	2.4
5	Type B 1.55	65.0	37.0	1.92	6.3	36.0	0.97	1.76	2.4
6	Type B 1.55	62.0	32.0	1.52	5.3	19.0	0.59	1.93	2.1
7	Type C 1.18	50.0	38.0	1.67	3.0	9.9	0.26	1.32	3.0
8	Type C 1.18	42.0	25.0	1.79	1.5	5.6	0.22	1.68	4.6
9	Type C 1.18	30.3	21.0	1.61	2.0	6.1	0.24	1.44	3.6

Cause of Surge Formation

The reason why Type B was formed at surge flow motion may be considered as follows;
One of the reasons may be caused by the gravel size sorting phenomenon in which the large gravels flow towards the front and the sand flows back behind the gravels as shown in Fig. 7.
The sorting phenomenon associated with the inverse grading phenomenon is explained as follows.
(1) The large gravels are transported to the front flow and dropped to the floor.
Bagnold (1968) proposed that this is based on the concept of dispersion pressure due to the impact between two gravel particles. This means that the dispersion pressure is proportional to the gravel diameter to the 2nd power and, as such, large gravels are moved to the direction of the minimum shearing velocity, i.e., the direction of the upper free surface.
Middleton (1970) opposed Bagnold's remark that small gravels are dropped down to the floor and the large gravels go up to the upper surface by the dynamic sieving effect.

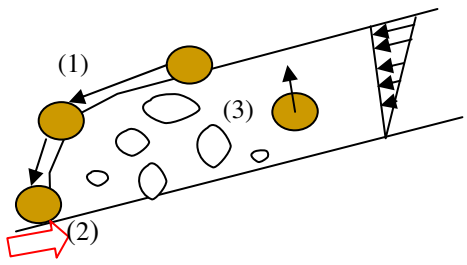

Fig.7 Sorting phenomenon of gravel and sand

On the otherhand, Takahashi (1980, 2004) explained that the large gravels are transported to the front flow as if the soil attached to the bulldozer were jumped to the front direction rather than the moving

velocity of the bulldozer itself, because the upper flow velocity is faster than the lower one in the flow depth direction. This means that the gravel distribution was rearranged into the large gravel and sand.
(2) The friction between gravel and floor makes the flow velocity slow at the bottom and gives resistance to the flow motion. Therefore, the dropped large gravels are left behind on the floor because of the slow fluid velocity in the depth direction.
(3) However, the large gravels are again pushed up to the upper surface due to the dynamic sieving effect mentioned above. That is, small gravels and sand are transported to the back and large gravels are conveyed to the upper surface. This phenomenon is the sorting or rearragement of sand and gravel.
Consequently, Type B was suited for the surge formation, because of satisfying the conditions (1)-(3) within the range in this test.

DYNAMIC RESPONSE TEST

Outline of test

The dynamic response test under debris models was performed for Sabo dam model which was made by steel plates with a length of 300mm, a width of 100mm and thickness of d=0.5mm and 2.0mm, respectively.The dynamic response of mortar plates was also examined by using the plates with a length of 300mm, a width of 100mm and thickness of d=5mm and 10mm, respectively, in order to compare with a steel plate. The steel and mortar plates were fixed in the bottom as the cantilever plate in which the deformation and strains were measured as shown in Fig. 4.

Test results

(1) The strain-time relation of a steel plate under Type B was obtained as shown in Fig.8. It was found that the maximum strain showed at the h=5cm from the bottom of steel plate.in Fig.4, because the steel plate behaves as a flexural action of cantilever plate.

(2) The comparison between the maximum strain-time relations of Types A, B and C is illustrated in Fig.9, where the maximum strain is measured at 5cm from the bottom. It was found that the debris flow surge model of Type B gives remarkable influence on the maximum strain, but Types A and C did not so much effect on the maximum strain.

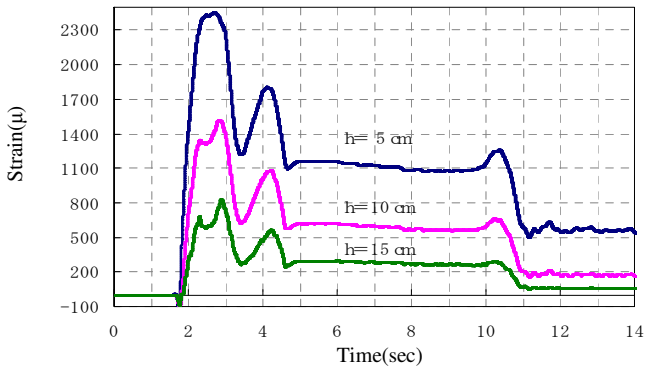

Fig.8 Strain-time relation of steel plate (d=0.5mm)

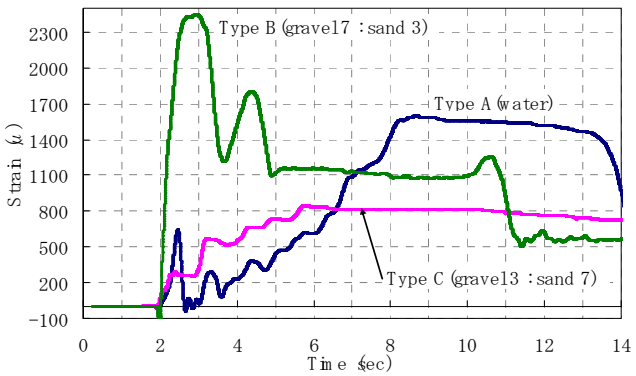

Fig. 9 Maximum strain-time relation of Types A,B,C (steel plate :d=0.5mm)

(3) The effect of thickness of steel plates (d=0.5mm and d=2.0mm) under Type B is examined as shown in Fig.10. It was confirmed that the dynamic response may be significantly reduced about 1/8, if the thickness of the plate is increased about 4 times.

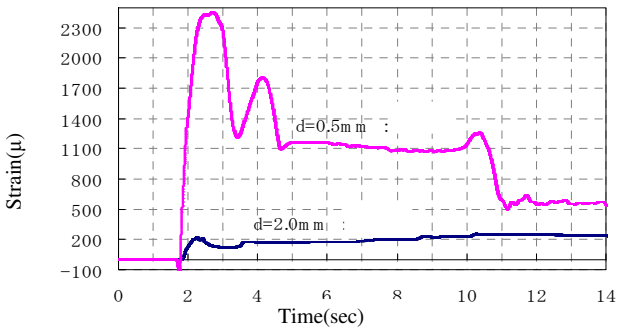

Fig.10 Effect of steel plate thickness (Type B)

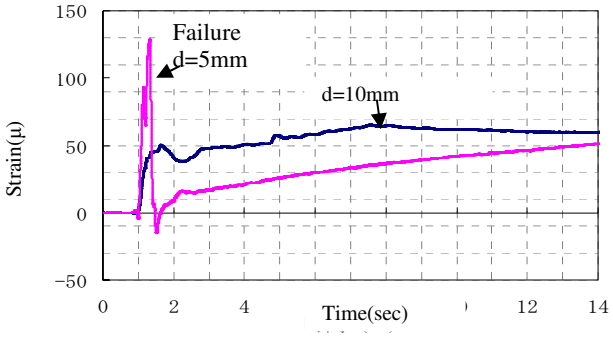

Fig.11 Effect of mortar plate thickness (Type B)

(4) The deformation profile of the steel plate with thickness d=0.5mm under Type B is illustrated in Fig.12. It was found that the steel plate behaved as ductile materials which was not collapsed by the flexural action of a cantilever, even a thin steel plate

(5) The effect of thickness of mortar plates (d=5mm and 10mm) under Type B is investigated as shown in Fig.11 in order to compare with a steel specimen. It was found that the mortar plate collapsed at the bottom in the case of thickness d=5mm as shown in Fig.13, although d=5mm of the mortar plate is 10 times larger than d=0.5mm of the steel plate. This phenomenon may be due to the brittle materials of mortar. However, the mortar plate with the thickbess d=10mm did not fail in the inelastic state.

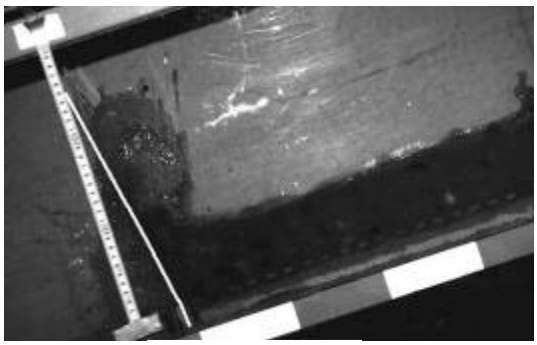

(a) t=2.10sec

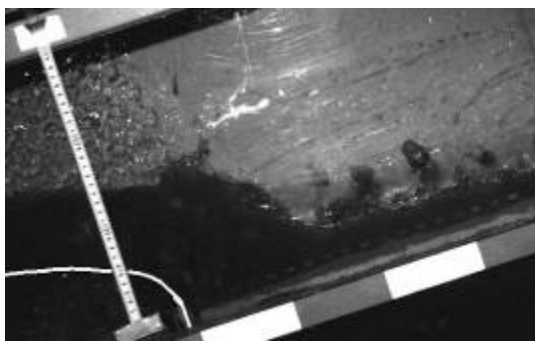

(b) t=2.55sec

Fig.12 Deformation profile of steel plate (d=0.5mm) (Type B)

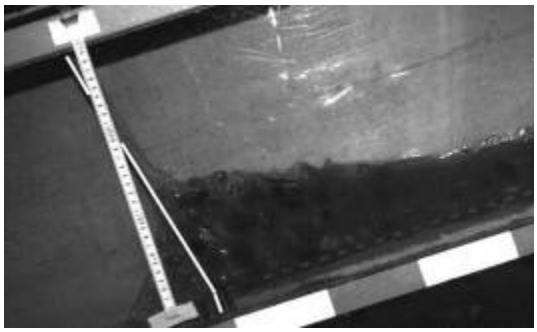

(a) t=1.51sec

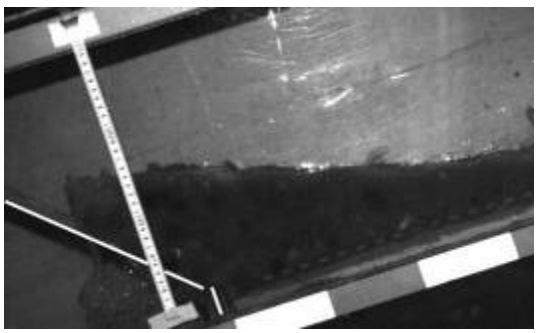

(b) t=1.62sec

Fig.13 Deformation profile of mortar plate (d=5mm) (Type B)

Outline of Computational Method

The dynamic response analysis is performed by using the MPS (Moving Particle Semi-implicit) Method (Koshizuka, 2005) with a deformation analysis of a steel plate under water flow (Type A). Herein, the MPS method was combined with the deformation analysis of a cantilever plate which is assumed as a beam elment as shown in Fig.14. First, the dynamic water pressure of plate is calculated by using the MPS method. Then, the deformation analysis based on the beam theory is performed for a plate subjected to the dynamic water pressure. As the results, the plate is bent by the water pressure. Third, the bent plate is again subjected to the water pressure and continues the calculation of deformation analysis until the flow ends.

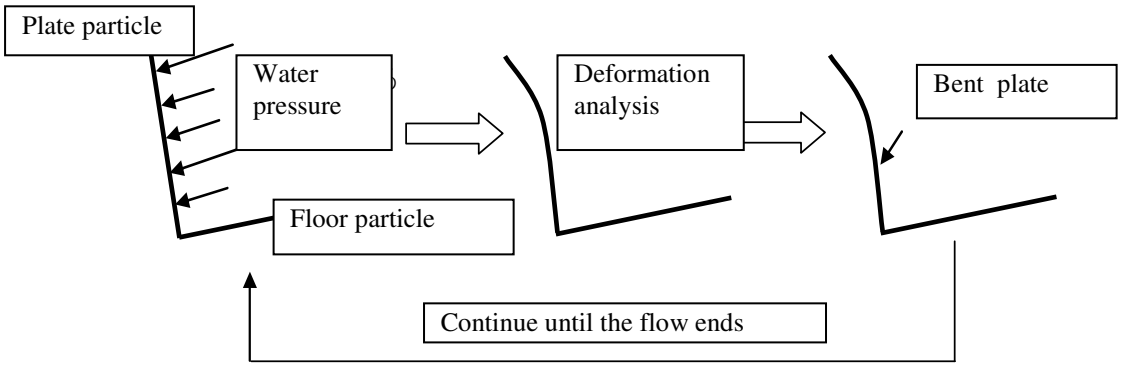

Fig. 14 Outline of deformation analysis of plate (beam element)

The initial condition of water flow is set as the washout height of 15cm and the channel slope of 18 degree as shown in Fig.15. In order to consider the viscosity of water, the dynamic viscous coefficient ν_ℓ =5.0×10^{-2}mm^2/ms is used between two water particles and $\nu_{\ell s}$ =1.0×10^{-2}mm^2/ms is used for water and floor interaction.

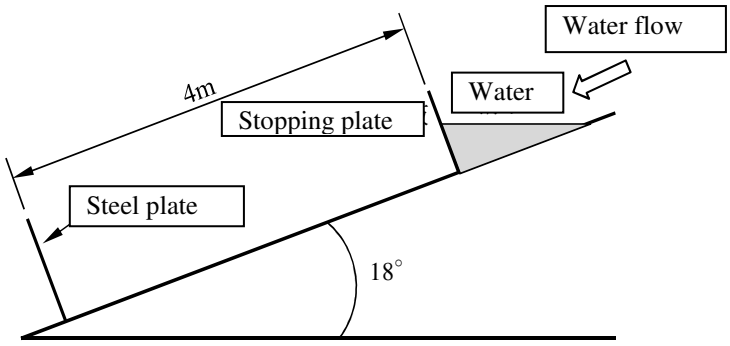

Fig.15 Dynamic response analysis of steel plate under water flow

Simulation Results

(1) The computational flow motion is obtained as shown in Fig.16 which is compared with the test flow motion as shown in Fig.6(a). It is found that the flow motion by analysis is almost similar to the test result, although the front particles are dispersed by the impact to the steel plate.

(2) The pressure-height relation of steel plate under Type A is shown in Fig.17. It is found that the maximum pressure occurs at the bottom of plate, because the water hit the bottom of plate at the first time. Therfore, it was confirmed that this paricle method simulated well the fluid-plate interaction.

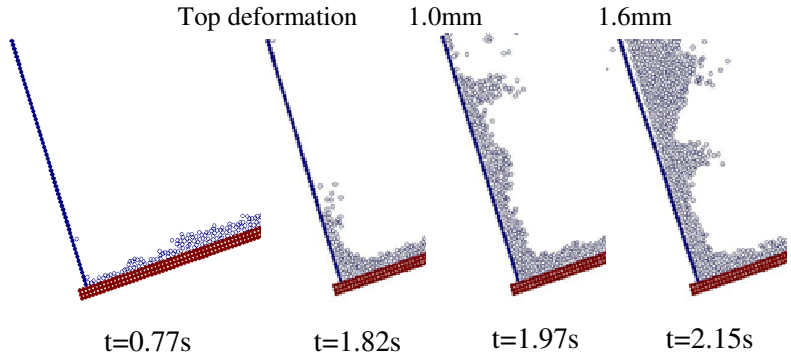

Fig. 16 Deformation profile of steel plate (d=0.5mm)

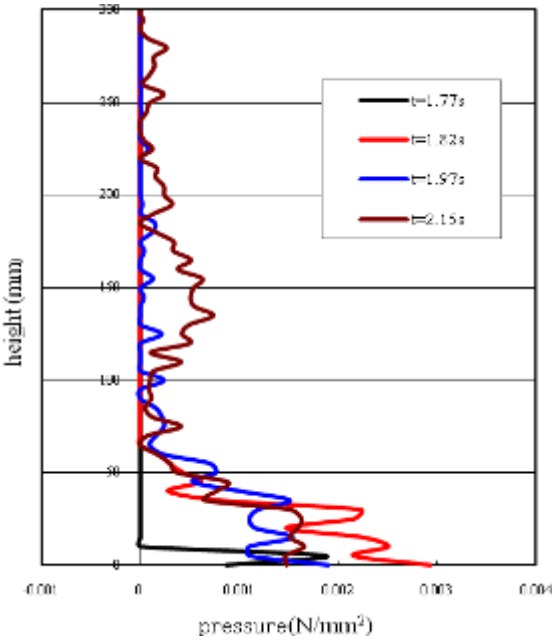

Fig.17 Pressure-height relation of steel plate (Type A)

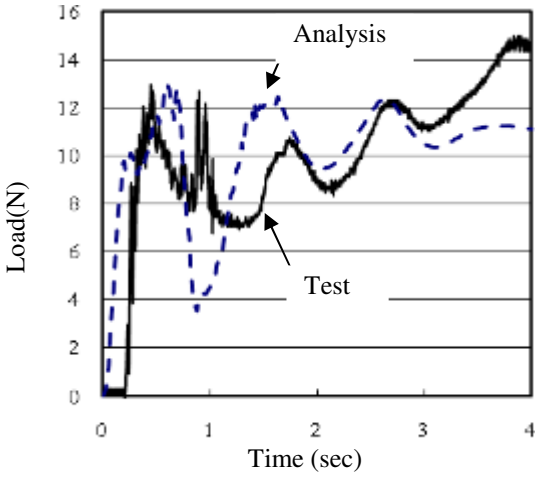

Fig.18 Load-time relation (Type A)

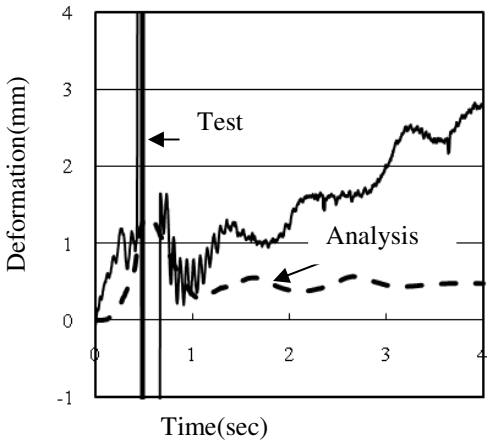

Fig.19 Deformation-time relation(Type A)

(3) The load-time relation by analysis is illustrated in Fig.18 comparing with the test result. It is noted that the maximum load by analysis is about 13N and is almost in good agreement with the test result.

(4) The deformation- time relation by analysis is shown in Fig.19 comparing with the test result. It is interesting that the deformation by test at the time of 0.5sec became to the infinity, because the laser type deformation sensor was splashed by the water flow and could not measure the deformation. However, the maximum deformation by analysis was about 1.2mm at the time of 0.6sec, although it was not so good agreement with the test data after the time of 1sec, because the successive flow water was not considered in the deformation analysis.

(5) The strain–time relation is represented in Fig.20 at the point of h= 5cm from the bottom of plate.

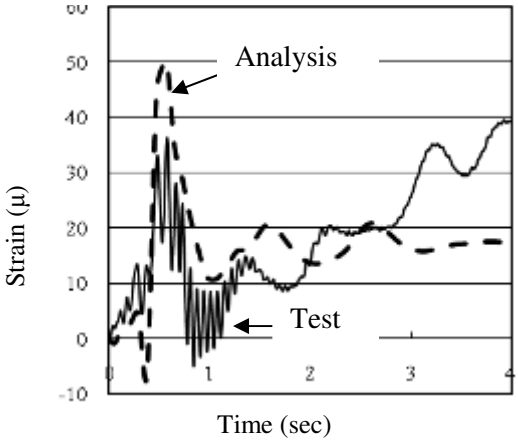

Fig.20 Strain-time relation of h=5cm (Type A)

It is recognized that the maximum strain shows 50μ by analysis which is greater than 38μ of test. However, the general strain-time curve by analysis is
almost in good agreement with the test result.
Therefore, the proposed dynamic response analysis can simulate well the dynamic load, deformation and strain-time relations of a steel plate by using the MPS method combining with the deformation analysis based on the beam theory.

CONCLUSIONS

The following conclusions are drawn from this study.
(1) It was found that surge shape was well formed in Type B
(70% gravel of and 30% sand) in which the load-time relation shows a very steep rise time and the impulsive peak load.
(2) It was recognized that the design load almost coincides with the constant load after the peak load in Types A and B.
(3) The maximum strain showed at the bottom of plate, because this fact may be caused by the flexural action of a steel plate.
(4) The maximum strain of a steel plate under Type B showed the large dynamic response of steel plate, as this phenomenon was caused by the impulsive load due to the surge formation of debris flow.
(5) It was confirmed that the dynamic response of the steel plate was significantly reduced by increasing the thickness of the plate.
(6) It was also found that the mortar plate with thickness of 5mm failed at the bottom of plate under Type B. This may be due to the brittle materials, even if the thickness of mortar plate is 10 times larger than the one of steel plate.
(7) As the results of the dynamic load and dynamic deformation analyses of the steel plate under flow water, the particle method (MPS method) can simulate well the dynamic response of a steel plate.
Therefore, this method will be useful tool for the investigation of dynamic response of a Sabo dam structure under debris flow.

REFERENCES

Bagnold R.A. (1968). Deposition in the process of hydraulic transport. Sedimentology,10, pp.45-56.

Bugnion L., McArdell B., Bartelt P., Wendeler C. (2011). Measurements of hill slope debris flow impact pressure on obstacles. Landslides , (10 September), pp. 1-9.

Daido J. (1988). Impact load of debris flow acting on Sabo dam. Proc.of Sabo Society Meeting, pp.275-276. (in Japanese).

Hirao K., Tenda K., Tabata S., Matsunaga M. and Ichinose E. (1977). Fundamental test on the impulsive pressure of surge (Part 1). Journal of Shin-Sabo, Vol.76, pp.11-16. (in Japanese).

Horii N., Toyosawa Y., Tamate S. and Hashizume H. (2002). Experimental study on flow characteristics of debris flow. Special Research Report of Industrial Safety Institute, No.25, pp.17-23.(in Japanese).

Hu K., Wei F. and Li Y. (2011). Real-time measurement and preliminary analysis of debris-flow impact force at Jiangjia Ravine, China. Earth Surface Processes and Landforms, Vol.36, Issue 9, pp. 1268–1278, John Wiley & Sons, Ltd.

Ishikawa N., Inoue R., Hayashi K., Hasegawa Y. and Mizuyama T. (2008). Experimental approach on measurement of impulsive fluid force using debris flow model, Conference Proceedings of INTERPRAEVENT, Vol.1, pp.343-354.

Ishikawa N., Inoue R., Beppu M., Hasegawa Y. and Mizuyama T. (2009). Impulsive loading test of debris flow model. Proc.of the 8th International Conference on Shock & Impact Loads on Structures, pp. 53-62, Adelade,Australia.

Ishikawa N., Inoue,R., Beppu,M., Hasegawa,Y., and Mizuyama,T. (2010). Dynamic characteristics of debris flow model using different gravel size distribution. Symposium Proceedings of INTERPRAEVENT 2010, pp.207-216.

Koshizuka S. (2005). Particle Method, Computational Mechanics. Series 5, Maruzen Press. (in Japanese).

Middleton G.V. (1970). Experimental studies related to problems of flysch sedimentation. Lajoie J.ed., Flysch Sedimentology in North America, Geology Association of Canadian Specification, Paper 7, pp.253-272.
Mizuyama T. (1979). Evaluation of debris flow impact on Sabo dam and its problems. Journal of Shin-Sabo, 112, pp.40-43.(in Japanese).
Mizuyama T., Shimohigashi H., Nakanishi H. and Matsumura K. (1985). Experimental study on debris flow loads for steel slit type Sabo dam. Journal of Shin-Sabo, Vol.37, No.5, pp.30-34. (in Japanese).
Miyamoto K. and Daido J. (1983). A study on impact load acting on Sabo dam (Part 1). Memoirs of Science and Engineering Institution of Ritsumeikan University, Vol.41, pp.61-79. (in Japanese).
Miyoshi I. and Suzuki M. (1990). Experimental study on impact load of debris flow. Journal of Shin-Sabo, Vol.43, No.2, pp.11-19. (in Japanese).
Takahashi T. (1980). Debris flow on prismatic open channel. Journal of Hydraulic Engineering, ASCE, 106, NoHY3, pp.381-396.
Takahashi T. (2004). Mechanism and measure of debris flow. Kinmirai-sha, pp.175-184, (in Japanese).